Glycosyl-Curcuminoids as Potential New Chelating Agents in Iron Overload Chelation Therapy

Beatrice Arezzini,[a] Marco Ferrali,[a] Erika Ferrari,[b] Romano Grandi,[b] Stefano Monti,[b] and Monica Saladini*[b]

Keywords: Chelates / Iron / Gallium / Redox chemistry / Bioinorganic chemistry

The iron(III) chelating ability of some glycosyl derivatives of curcuminoids is tested by means of UV, potentiometric and NMR studies. The pK_a of the ligands and the stability constants of their Fe^{3+} and Ga^{3+} complexes are evaluated by UV spectroscopy. The only metal binding site of the ligand is the β-dioxo moiety; the glycosyl moiety does not interact with the metal ion at acidic pH values but it helps to stabilise metal/ligand (1:2) complexes by means of hydrophilic interactions. By comparing the pFe^{3+} of our ligands with those reported for other chelating agents we suggest using these molecules as pro-drugs in iron overload treatment. Some of the more water-soluble derivatives are also tested for their antioxidant properties "in vitro" in biological systems and proved to act as free-radical scavengers inhibiting the iron redox cycle.

Introduction

Iron regulation in the human body follows complex mechanisms that tend to limit external exchange and make the re-utilisation from internal sources more efficient. However, although essential for the proper functioning of living cells, iron is toxic when present in excess. In the presence of oxygen, "loosely bound iron" is able to switch between its two more stable oxidation states (Fe^{3+}/Fe^{2+}), thereby generating hydroxyl radicals and favouring the so-called "Fenton Chemistry".[1,2] In healthy individuals, iron levels are under tight control and there is little or no opportunity for iron-catalysed free radical generating reactions. However, there are situations where the iron status can change, either locally, as in ischaemic tissue, or systematically, as with genetic haemochromatosis or transfusion-induced iron overload, as for patients suffering from β-thalassemia. So it is intuitively derived that metal — in this particular case iron — intoxication should be treated with chelating agents.

The main feature of the design of a chelating agent for iron should be its affinity and selectivity towards this metal. The most widely used iron chelator is Desferrioxamine B (Desferal®, DFO), a hexadentate ligand from the family of siderophores that shows great affinity for iron(III), giving rise to a 1:1 complex. The main drawback of DFO, apart from side effects with prolonged treatment, is that it has to be administered by intravenous injection. Consequently, there is an urgent need for an orally active chelating agent able to improve the way of life of patients.

The main target in designing an orally active sequestering agent is its bio-availability, which is related to an efficient gastrointestinal tract (GIT) absorption. The ligand needs to be quite lipo-soluble in order to be absorbed by the gastrointestinal tract, although this property also enables it to penetrate critical barriers such as the blood-brain barrier (BBB) and the blood-placental barrier (BPB). A possible way to overcome the negative aspects of lipophilicity is to use a lipophilic pro-drug that is easily absorbed by the GIT and reach the bloodstream, where it can be cleared by the liver and finally converted into an iron-selective chelator in the hepatocytes. The complex formed by iron scavenging inside the hepatocytes can be excreted by bile and/or urine.

Curcumin is spice and pigment from *Curcuma longa* L. (Zingiberaceae) and it is best known for its antioxidant,[3–6] anti-inflammatory[4,7] and anticancer[3,4,8,9] activities. We have recently investigated the iron-chelating ability of curcumin and its diacetyl derivative (Scheme 1), observing a lowering of the pK_a value of the β-dioxo moiety in the presence of iron(III), and the formation of mixed hydroxo species ($[Fe(CURH_2)(OH)_2]$ and $[Fe(DCUR)(OH)_2]$) in a methanol/water (1:1) solution, whose stability is close to that of the Desferrioxamine complex. The main drawback in the clinical use of curcumin is its low water solubility. To overcome this handicap, we have synthesised new glycosyl

[a] Department of Physiopathology and Experimental Medicine, University of Siena,
Via Aldo Moro, 53100 Siena, Italy
E-mail: ferrali@unisi.it
[b] Department of Chemistry, University of Modena and Reggio Emilia,
Via Campi 183, 41100 Modena, Italy
E-mail: saladini@unimore.it
Supporting information for this article is available on the WWW under http://www.eurjic.org or from the author.

  DOI: 10.1002/ejic.200300463

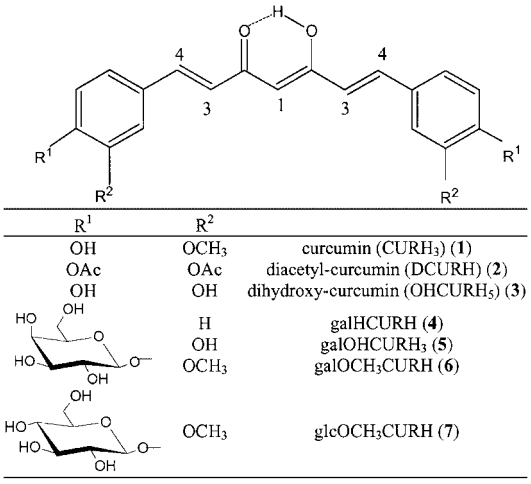

R^1	R^2	
OH	OCH_3	curcumin ($CURH_3$) (**1**)
OAc	OAc	diacetyl-curcumin (DCURH) (**2**)
OH	OH	dihydroxy-curcumin ($OHCURH_5$) (**3**)
	H	galHCURH (**4**)
	OH	$galOHCURH_3$ (**5**)
	OCH_3	$galOCH_3CURH$ (**6**)
	OCH_3	$glcOCH_3CURH$ (**7**)

Scheme 1

derivatives (Scheme 1). Apparently hexadentate ligands are the best iron chelators, and a recent study on a hydroxypyridinone derivative CP502 has shown good oral absorption and iron excretion, even though it is bidentate.[17] Glycosyl-curcuminoids have the great advantage of being administrated by oral formulation in their acetylated form, and even though their high molecular weight hinders the diffusion processes through the GIT, high dosages are completely safe. Acetyl-glycosyl-curcuminoids can probably be absorbed by the GIT thanks to their high lipophilicity. They then reach the liver where, through hydrolytic processes, the glycosyl-curcuminoids are set free to complex iron and then excreted in urine and/or bile.

Here we investigate by means of spectroscopic (UV/Vis and potentiometric) techniques the iron(III) and gallium(III) chelating ability of these ligands; NMR spectroscopic data are also useful in studying the metal complexation, therefore we substituted the paramagnetic iron(III) with diamagnetic gallium(III) as suggested in some recent works.[10−12] Some of the water-soluble derivatives were also tested for their antioxidant properties "in vitro" in a biological system.

Results and Discussion

Potentiometry

The low water solubility of compounds **1**−**6** ($\leq 5 \times 10^{-5}$ M) prevented the potentiometric analysis of these systems. The greater solubility of **7** (approx. 5×10^{-3} M) allowed us to perform a potentiometric study and the evaluated data are reported in Tables 1 and 2, together with the spectrophotometric data. Potentiometric analysis gives more accurate results than the other techniques but the stability constants' values are very similar to those calculated from the UV data, therefore we may consider spectrophotometric analysis a reliable probe in testing the chelating ability of slightly water soluble systems.

Table 1. Logarithm of stepwise protonation constant (estimated standard deviation 0.1, if not specified); T = 25 °C, I = 0.1 M $NaNO_3$

	3[a]	**4**	**5**	**6**	**7**
$\log K_{a1}$	7.8	8.8	7.9	9.2	9.2/9.22(3)[b]
$\log K_{a2}$	8.6		9.9		
$\log K_{a3}$	9.3		10.9		
$\log K_{a4}$	10.8				
$\log K_{a5}$	12.5				

[a] $\log K_a$ values are referenced to a methanol/water (1:1) system. [b] Potentiometric data.

Table 2. Logarithm of stability constants of complex species calculated from spectrophotometric and potentiometric data for iron(III) and gallium(III) complexes; all data recorded at 25 °C, I = 0.1 M $NaNO_3$; estimated standard deviation of 0.1 if not specified; L represents the ligand with the enolic group in the dissociated form

	4	**6**	**7**	**7**[a]	**5**	**3**[b]
$[FeL]^{2+}$	10.2	10.7	11.0	10.73(3)	10.3	17.1
$[FeL(OH)]^{+}$	1.7	2.8	2.4	2.98(2)	0.3	20.8
$[FeL_2]^{+}$	19.5	20.5	20.8	19.82(1)	22.7	
$[FeL_2(OH)]$	13.2	16.3	16.0	16.10(2)	13.5	
$[GaL]^{2+}$	9.8	12.1	11.8		11.2	
$[GaL(OH)]^{+}$	3.7	2.8	3.2		1.2	
$[GaL_2]^{+}$	19.0	22.9	22.5		19.0	
$[GaL_2(OH)]$	14.0	14.2	12.5		10.5	

[a] Potentiometric data. [b] $\log\beta$ values are referenced to a methanol/water (1:1) system.

UV/Vis Spectroscopy

Glycosyl-curcuminoids, similarly to curcuminoids, maintain their dye properties — they are all characterised by an absorbance at ca. 400 nm.

Upon plotting absorbance vs. pH, only one equivalent point is observed for each ligand; the pK_a values calculated from the spectrophotometric data are reported in Table 1. The presence of the sugar moiety does not affect the pK_{a1} value, while some electronic effect is due to the substituents on the aromatic ring: the electron-withdrawing effect of OH groups stabilizes the conjugate base, lowering the pK_{a1} value, and as a consequence ligand **5** is the most acidic one in aqueous solution.

The addition of an iron(III) solution to the free ligands causes an LMCT[13] band to appear at ca. 500 nm, typical of (β-diketonate)Fe^{3+} complexes, and by monitoring the changes in the spectra upon progressive addition of Fe^{3+} solution, the stoichiometry of the complexes can be proposed.

Figure 1 shows the absorbance increase with the M/L molar ratio, which reaches a maximum at an M/L value of 0.5, corresponding to an M/L (1:2) complex. Once the 1:2 complex has formed no more significant changes in ab-

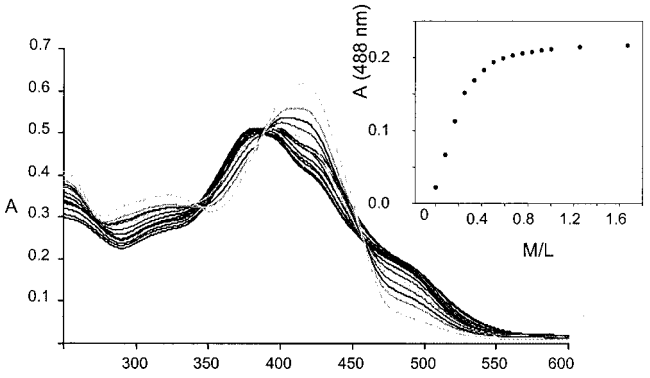

Figure 1. Spectrophotometric titration of **5** with Fe^{3+} solution and plot of absorbance vs. M/L at λ = 488 nm

sorbance are seen for the LMCT band, probably due to the small difference in the spectrophotometric curves of the 1:1 and 1:2 complexes. The addition of metal solution, causing a reduction in the pH value from 5 to 3, induces the formation of complex species even at a pH of about 3. The same experiments were carried out under buffered conditions (pH = 7), where the only difference is the increased intensity of the LMCT band. No differences were found in logβ values when taking into account the formation of a phosphate complex as its stability ($\log K[FeHL]^+ = 7.5$[14]) is significantly lower than those of our complexes.

Titration of the ligands with Ga^{3+} solution generates the same behaviour as observed in the presence of Fe^{3+}.

The pH-metric titration of the metal complexes was performed in aqueous solution for the glycosyl derivatives, while for the **3**/Fe^{3+} system a methanol/water (1:1) solution was used due to the poor solubility of the ligand in aqueous media. No hint of metal complex or metal hydroxide precipitation was observed.

The pH-metric titration of all L/Fe^{3+} (1:1) systems gives a typical UV spectral pattern and a plot of λ_{max} vs. pH, or *A* vs. pH at fixed λ gives a titration curve with two equivalent points (EP; Figure 2). The first EP (pH ≈ 4) is due to the deprotonation of the β-dioxo moiety, although it is several pH units lower than normal thanks to the great affinity for Fe^{3+}. The second one is probably due to the cleavage of

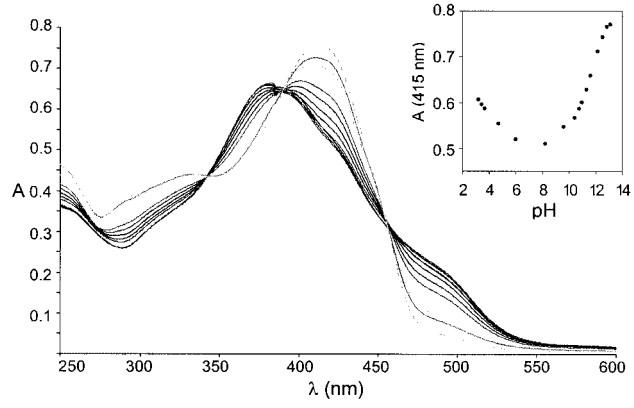

Figure 2. Spectrophotometric titration of a **7**/Fe^{3+} (1:1) system with NaOH and plot of absorbance vs. pH at λ = 415 nm

the metal complex under extremely basic conditions (pH > 10) and to the competition of hydroxide anions in metal complexation, although in **3**- and **5**-containing systems the involvement of dissociated catechol groups in metal coordination cannot be excluded.

The pH-metric titration of Ga^{3+}-glycosyl-curcuminoids parallels well the performance in the presence of Fe^{3+}.

The stability constants for Fe^{3+} and Ga^{3+} complexes are reported in Table 2. Comparison of the behaviour of glycosyl-curcuminoids with those of the parent curcuminoids shows that the former prefer M/L (1:2) complexes despite the steric hindrance of the saccharide units. This is because of the polar/non-polar character of the molecule. In aqueous solution the apolar core is tightly bound to the metal ion while the polar units form hydrophilic interactions (especially hydrogen bonds), giving a more stable structure and hindering the metal ion from coordinating additional ligands such as oxygen, therefore probably inhibiting oxidative processes.

In order to compare stability constants relative to the same kind of equilibrium, they need to be corrected by considering the ligand's protonation constants. It is more useful to consider the species distribution to understand which is the prevailing species under physiological conditions. In Figures 3−5 the species distribution curves for **7**/Fe^{3+}-, **5**/Fe^{3+}- and **3**/Fe^{3+}-containing systems are reported.

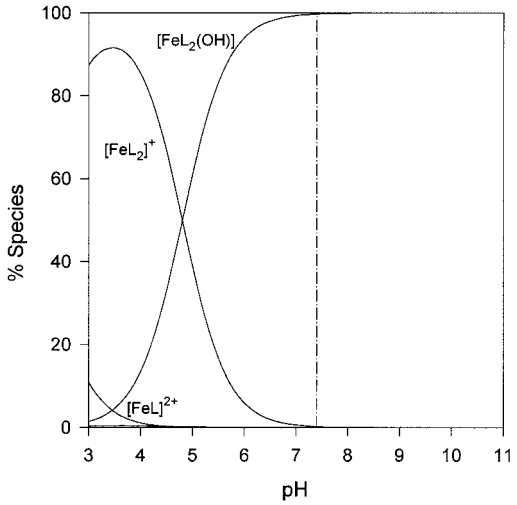

Figure 3. Species distribution curves for Fe/L systems in a 1:4 molar ratio; $[Fe^{3+}] = 5 \times 10^{-5}$ M, L = **7**

The prevailing species at physiological pH (7.4) have different stoichiometries for the three classes of ligands reported. Therefore a more proper comparison of the effective Fe^{3+}-chelating ability is represented by pFe^{3+}, defined as $-\log[Fe^{3+}]$.[15] This value is usually calculated with [L] = 10^{-5} M and $[Fe^{3+}] = 10^{-6}$ M, and, unlike stability constants, takes into account the effects of ligand protonation and denticity as well as differences in metal/ligand stoichiometry. A plot of pFe^{3+} versus pH provides a useful method for comparing the ability of chelators to bind iron(III) at different pH values as a high value of log*K* is not necessarily characterised by a high value of pFe^{3+}. Figure 6

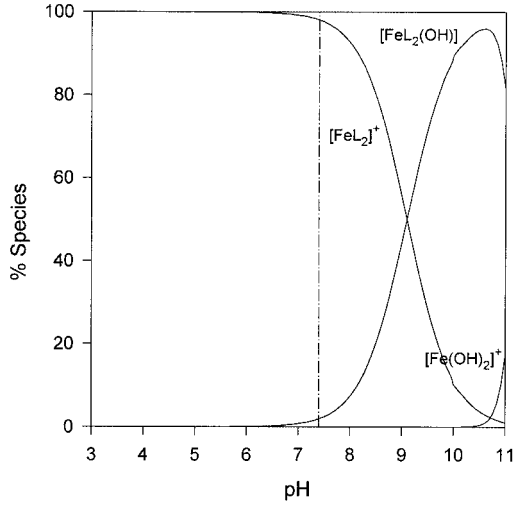

Figure 4. Species distribution curves for Fe/L systems in a 1:4 molar ratio; $[Fe^{3+}] = 5 \times 10^{-5}$ M, L = **5**

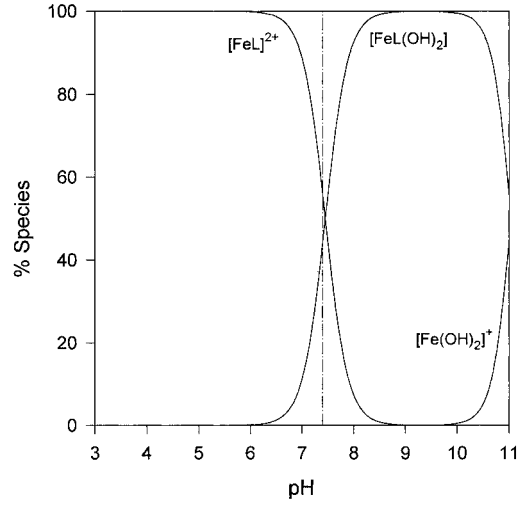

Figure 5. Species distribution curves for Fe/L systems in a 1:4 molar ratio; $[Fe^{3+}] = 5 \times 10^{-5}$ M, L = **3**

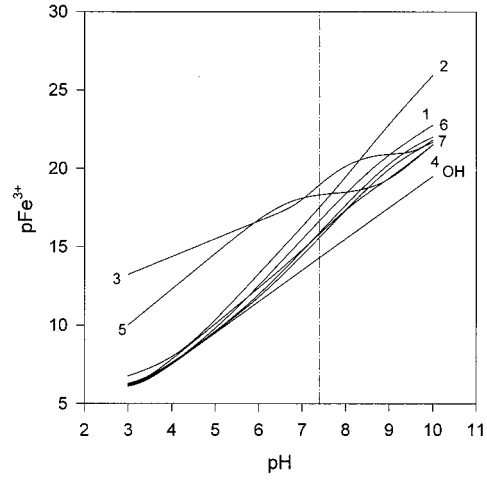

Figure 6. pFe^{3+} vs. pH for curcuminoids and glycosyl-curcuminoids; $[Fe^{3+}] = 10^{-6}$ M, [L] = 10^{-5} M; OH stands for Fe^{3+} aqueous solution

shows the plot of pFe^{3+} vs. pH for the curcuminoids and glycosyl-curcuminoids investigated in this work. Compounds **3** and **5** show the highest pFe^{3+} values at physiological and acidic conditions, despite their low $\log K_{a1}$ values; this behaviour may be due to the presence of phenolic functions that play an important role in the hydrogen bond network involving water molecules, and furthermore they are possibly involved in metal interactions. Table 3 shows the pFe^{3+} for different chelating agents. Notice how hexadentate ligands usually have higher pFe^{3+} values than bidentate one.

Table 3. pFe^{3+} values at pH = 7.4 for different Fe^{III}-chelating agents; DFO = Desferoxamine; DMB = 2,3-dihydroxy-*N*,*N*-dimethylbenzamide

	pFe^{3+}
MECAM[a]	28
DFO[a]	26
3-Hydroxypyridin-4-one[a]	20
3	19.0
5	18.3
2	17.6
1	16.7
6	15.9
4	15.8
7	15.6
DMB[a]	15
Acetohydroxamic acid[a]	13

[a] Values taken from ref.[33]

NMR Study

All spectra of glycosylated ligands are characterised by a sharp distinction between the pyranoside moiety and the aliphatic and aromatic ones; of particular interest are the protons on the double bond and the enolic proton, although the latter is quite mobile and tends to exchange in MeOD solution with D_2O. Gallium(III) can properly substitute iron(III) for the NMR study.[11−13] The study of its interactions in solution is useful in order to understand both the real chelating site and the stoichiometry of the complexes.

Titration of a solution of **5** with Ga^{III} (Figure 7) indicates the formation of new signals, in slow exchange on the NMR timescale, upon increasing the M/L molar ratio. The titration was performed without any buffer, since little changes are observed in the pH values (ca. 0.5 pH units). The formation of the new sets of signals is not a consequence of the pH decreasing induced by hydrolysis of Ga^{III}, but it is more reasonably attributed to the formation of complex species.

On increasing the Ga^{III} concentration the first kind of complex is formed; all of the ligand is complexed when the ratio mol of metal/mol of ligand is 0.5, therefore a 1:2 stoichiometry can be proposed for this species. The greatest downfield shift is for the 4-H signal; 4-H probably "feels" the positive charge in the resonance structure of the bis-

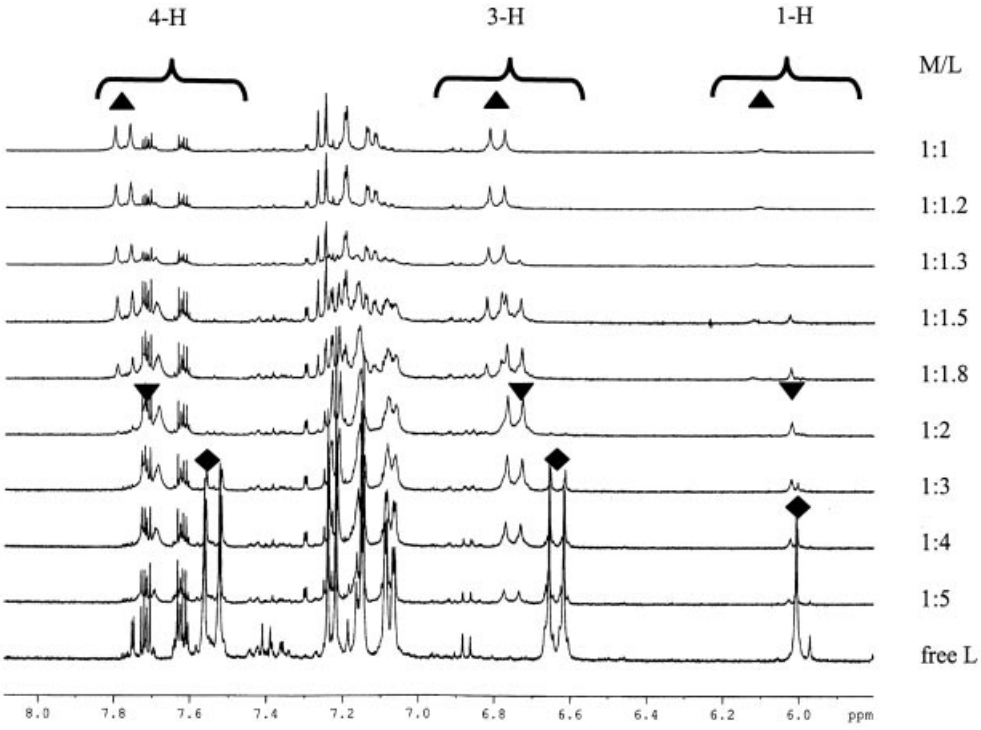

Figure 7. ^{1}H NMR titration of **5** with $Ga(NO_3)_3$ in MeOD solution; diamonds: free ligand signals; downward pointing triangles: M/L (1:2) complex signals; upward pointing triangles: M/L (1:1) complex signal

(chelate) complex, while a smaller shift is seen for the 3-H signal. Because of exchange processes with residual D_2O, the signal for 1-H is quite broad, making it difficult to follow its shift. Another important aspect of this titration is that the pH* value on the methanol scale is very low (ca. 2.5), and no addition of base is necessary to form the complexes, thus all these complex species are also present under very acidic conditions, and the affinity for metal ion is so high that it anticipates enolic deprotonation until pH* $\approx$ 3.

Upon increasing the quantity of metal further, the M/L (1:1) complex is formed. Its signals are more downfield shifted than those of the 1:2 complex, and this behaviour is in line with a more localised positive charge at the metal centre in the 1:1 complex than in the 1:2 complex. In line with the behaviour of curcumin, the phenolic groups in **5** do not interact with the metal ion, at least under the very acidic conditions that prevent catechol dissociation. Small changes are found for the aromatic protons due to the delocalisation of the metal charge along the aliphatic chain and aromatic rings. Finally, no evidence of an interaction between the sugar moiety and metal ion is observed by NMR spectroscopy in acid media, although we cannot exclude a possible glycoside interaction with the metal ion under physiological conditions, as reported in the literature in the solid state.[16−18]

The carbon atoms parallel the protons' behaviour. 2D inverse detection methods show a greater shift of the C-4 signal (δ = 4 ppm) followed by the C-3 signal (δ = 2 ppm) in the 1:1 complex, while in the 1:2 complex smaller shifts are observed.

Attempts to titrate the 1:1 complex solution with NaOH resulted in precipitation of the metal complex.

All glycosyl-curcuminoids share the same behaviour, confirming that the substituents on the aromatic rings and the nature of the sugar do not affect the metal coordination.

Effect of the Chelators on Lipid Peroxidation

Figure 8 shows the time-dependent formation of TBARS as a hint of iron-dependent lipid peroxidation in rat liver microsomes. Notice that the presence of the chelators **3** and **5** interferes — although to different extents — with the lipid peroxidation evolution. In particular, compound **3** almost completely inhibits TBARS formation even if it is present in the incubation mixture at one half or the same concentration as that of the metal. On the other hand, compound **5** completely prevents microsomal lipid peroxidation only when present at a concentration twice that of iron. As a consequence, compound **5** seems to prevent TBARS formation only when the M/L (1:2) complex is formed, while compound **3** is active independently of the complexation stoichiometry. This is due to the catecholic structure of compound **3**, which possibly also acts as a free-radical scavenger when iron is present in excess compared to the chelator. It therefore seems to have a double action: it blocks oxygen-active species generated by the iron redox cycle and inhibits its initiation in the iron-chelated form. Since compound **5** is a galactosyl ester of compound **3** it is possible that under in vivo conditions, after galactosidase action, it acquires the same properties as **3**. In conclusion, both compound **3** and its derivative esters appear to be useful anti-

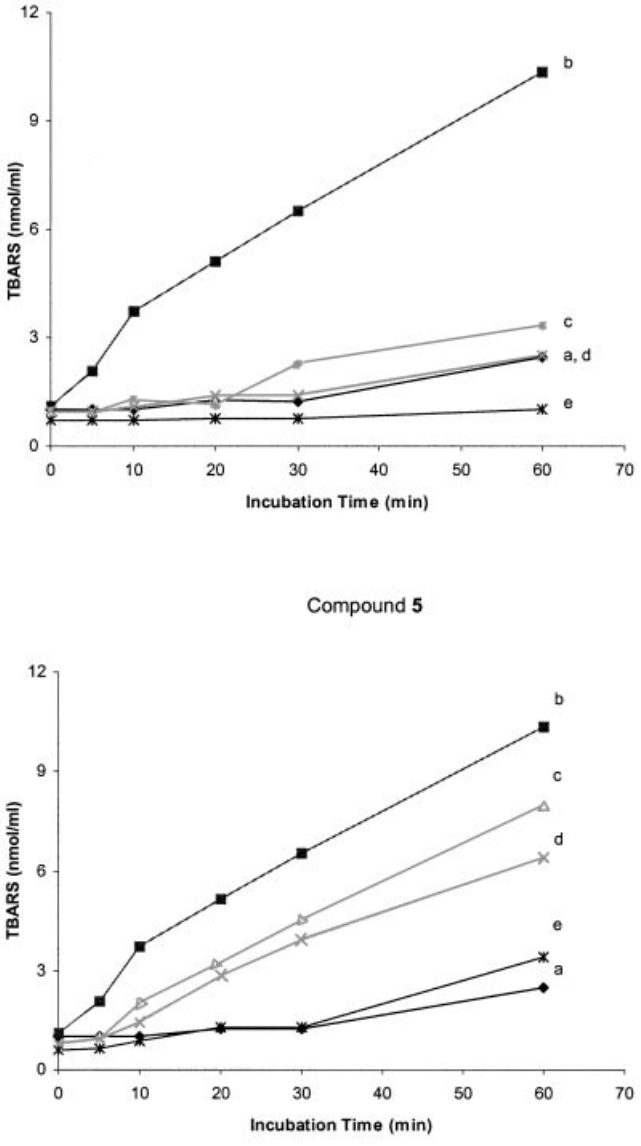

Figure 8. Iron-dependent TBARS evolution in a rat liver microsomal preparation (MC): a) control MC; b) MC plus 100 μM $FeCl_3$ and 2.5 mM ADP; c) as in b) plus 50 μM chelator; d) as in b) plus 100 μM chelator; e) as in b) plus 200 μM chelator; the microsomal protein concentration was 1.5 mg/mL in the incubation system; the values represent the mean of two or three experiments

oxidants preventing lipid peroxidation both in vitro and, presumably, in vivo.

Experimental Section

General: Compounds **4**−**7** were synthesised as reported in ref.[19], while compound **3** was synthesised according to the Pabon reaction.[20] $FeCl_3$ was used to avoid hydrolysis processes; standardisation of the stock methanolic solution was performed with a Spectroflame D ICP plasma spectrometer.

Potentiometry: Potentiometric measurements were performed in aqueous solution at 25 ± 0.1 °C according to the general procedures previously reported.[21] A constant ionic strength of 0.1 M (solid $NaNO_3$) and nitrogen gas were maintained in all experiments. The stability constants were refined with the Hyperquad program[22] taking into account the presence of $[Fe(OH)]^{2+}$ and $[Fe(OH)_2]^{+}$ species.[16] The protonation constant of the ligand was determined by the titration of 5×10^4 M solutions. The ligand/Fe system was investigated in 1:1, 1:2 and 1:4 molar ratios. Aqueous NaOH (5×10^{-3} M) was used as titrant in the pH range 3−10.

Spectroscopy: Spectrophotometric titrations were performed using a Perkin−Elmer Lambda 20 spectrophotometer at 25 ± 0.1 °C in the 200−600-nm spectral range, employing a 1-cm quartz cell. 2.5×10^{-5} M solutions of ligands **4**−**7** were investigated in aqueous solution while **3** was used in methanolic/aqueous (1:1, v/v) media; pH values were adjusted by adding small amounts of concentrated NaOH. In the titrations of **3** the glass electrode was calibrated using two appropriate buffers (pH = 5.57 and 8.02).[23] Constant additions (10 μL each time) of Fe^{III} solution (10^{-2} M) were performed using a micropipette in order to reach different M/L molar ratios. All the titrations were done also in a buffer solution (pH = 7.4, NaH_2PO_4/Na_2HPO_4). The pH-metric titration of the M/L (1:1) solutions was obtained varying the pH value by adding a small amount of concentrated NaOH. The protonation constants of the ligands and formation constants of metal complexes were evaluated from spectrophotometric titrations using the pHab2000 software.[24] ^1H NMR spectra were obtained with a Bruker Avance AMX-400 spectrometer at 400.13 MHz with a 5-mm broadband probe (inverse detection). Acquisition parameters were as follows: spectral bandwidth 17 ppm, pulse width 7.6 μs (90° pulse), pulse delay 1 s, number of scans 216−512. H,H COSY,[25] HMQC[26,27] and HMBC[28] were performed with typical averaged parameters: $^1J_{H,C} = 145$ Hz and $^3J_{H,C} = 7$ Hz, typical delay for inversion recovery optimised to give null for protons bound to ^{12}C, in BIRD sequence, is around 400 ms. The spectra of the ligands were recorded for mM solutions in CD_3OD, since their signals in D_2O solution were so broad that they could not be assigned, probably due to the formation of aggregate species. The combined electrode was standardised with CH_3OH buffers (pH = 5.79 and 7.53), pD values were then corrected by 0.4 units according to the relationship: pD = pH + 0.4.[25] All spectra were collected at 25 ± 0.1 °C and referenced to TMS. A solution of Ga^{III} was prepared by dissolving 2.5 mg of $Ga(NO_3)_3 \cdot 9H_2O$ in 0.1 mL of CD_3OD. Equimolar solutions of **3**−**7** in the same solvent were prepared. Constant additions (10 μL each time) of Ga^{III} solution were performed using a micropipette, the mixture was stirred and spectra were registered after a few minutes from the addition.

Biological Studies: Rat liver microsomes (MC) were prepared from fasted animals.[29] MC equivalent to 4 g of liver were resuspended in 36 mL of 50 mM trimaleate buffer (TM, pH = 7.4). The suspension was adjusted to 3 mg of microsomal protein per mL and 300 μM NADPH added just before the experimental procedure. A solution of 5 mM ADP plus 200 μM $FeCl_3$ was prepared in the same buffer. Solutions of ligands **3** and **5** (20 mM) in water/ethanol were prepared. To 3 mL of the microsomal suspension 0.6, 1.2, 2.4 μmol of the two chelators were added in separate flasks; then 3 mL of the ADP/iron solution was added and the incubation started at 37 °C in a shaking bath. After the indicated times, aliquots were withdrawn to measure the amount of TBARS formed.[30]

Supporting Information (see also footnote on the first page of this article): Figure showing the 2D heterocorrelated spectrum with evolution of the $^1J_{C,H}$ coupling constants for the free ligand **5**, the complex Ga^{III}-**5** (1:2) and the complex Ga^{III}-**5** (1:1); spectrophotometric titration of **5** (inset shows λ_{max} vs. pH).

Acknowledgments

We are thankful to the "Centro Interdipartimentale Grandi Strumenti (CIGS)" of the University of Modena and Reggio Emilia, which supplied the NMR spectrometer.

[1] B. Halliwell, J. M. C. Gutteridge, *Methods Enzymol.* **1990**, *186*, 1−85.
[2] H. C. Sutton, C. C. Winterbourn, *Free Radical Biol. Med.* **1989**, *6*, 53−60.
[3] Sreejayan, M. N. A. Rao, *J. Pharm. Pharmacol.* **1994**, *46*, 1013−1016.
[4] Sreejayan, M. N. A. Rao, *Int. J. Pharm.* **1993**, *100*, 93−97.
[5] M. K. Unnikrishnan, M. N. A. Rao, *Pharmazie* **1995**, *50*, 490−492.
[6] H. P. T. Ammon, M. A. Wahl, *Planta Med.* **1991**, *57*, 1−7.
[7] R. J. Anto, G. Kuttan, K. V. D. Babu, K. N. Rajasenkaran, R. Kuttan, *Pharm. Pharmacol. Commun.* **1998**, *4*, 103−106.
[8] R. J. Anto, G. Kuttan, K. V. D. Babu, K. N. Rajasekharan, R. Kuttan, *Int. J. Pharm.* **1996**, *131*, 1−7.
[9] H. H. Tønnesen, H. De Vries, J. Karlsen, G. B. van Henegouwen, *J. Pharm. Sci.* **1987**, *76*, 371−3.
[10] M. Borsari, E. Ferrari, R. Grandi, M. Saladini, *Inorg. Chim. Acta* **2002**, *328*, 61−68.
[11] R. A. Atkinson, A. L. M. S. El Din, B. Kieffer, J. F. Lefevre, M. A. Abdallah, *Biochemistry* **1998**, *37*, 15965−15973.
[12] Y. Hara, L. Shen, A. Tsubouchi, M. Akiyama, K. Umemoto, *Inorg. Chem.* **2000**, *39*, 5074−5082.
[13] S. Kazanis, T. C. Pochapsky, *J. Biomol. NMR* **1997**, *9*, 337−346.
[14] R. L. Lintvedt, L. K. Kernitsky, *Inorg. Chem.* **1970**, *9*, 491−494.
[15] H. H. Tønnesen, J. V. Greenhill, *Int. J. Pharm.* **1992**, *87*, 79−87.
[16] NIST Standard Reference Database 46, Critically Selected Stability Constants, Version 5, webbook.nist.gov
[17] R. C. Hider, Z. D. Liu, S. Piyamongkol, *Transf. Sci.* **2000**, *23*, 201−209.
[18] K. Hegetschweiler, T. Kradolfer, V. Gramlich, R. D. Hancock, *Chem. Eur. J.* **1995**, *1*, 74−88.
[19] K. Hegetschweiler, L. Hausherr-Primo, W. H. Koppenol, V. Gramlich, L. Odier, W. Meyer, H. Winkler, A. X. Trautwein, *Angew. Chem. Int. Ed. Engl.* **1995**, *34*, 2242−2243.
[20] K. Hegetschweiler, M. Ghisletta, L. Hausherr-Primo, T. Kradolfer, *Inorg. Chem.* **1995**, *34*, 1950−1953.
[21] E. Ferrari, R. Grandi, S. Monti, M. Saladini, *Can. J. Chem.*, in press.
[22] H. J. J. Pabon, *Recl. Trav. Chim. Pay-Bas* **1964**, *83*, 379−386.
[23] M. Borsari, L. Menabue, M. Saladini, *Polyhedron* **1999**, *18*, 1983−1989.
[24] P. Gans, A. Sabatini, A. Vacca, *Talanta* **1996**, *43*, 1739−1753.
[25] D. D. Perrin, B. Dempsey, *Buffers for pH and Metal Ion Control*, Chapman and Hall, London, **1979**.
[26] P. Gans, A. Sabatini, A. Vacca, *Ann. Chim.* **1999**, *89*, 45−49.
[27] K. Nagayama, A. Kumar, K. Wuethrich, R. R. Ernst, *J. Magn. Reson.* **1980**, *40*, 321−334.
[28] A. Bax, R. H. Griffey, B. L. Hawkins, *J. Magn. Reson.* **1983**, *5*, 301−315.
[29] A. Bax, S. Subramanian, *J. Magn. Reson.* **1986**, *67*, 565−569.
[30] A. Bax, M. F. Summers, *J. Am. Chem. Soc.* **1986**, *108*, 2093−2094.
[31] M. Ferrali, S. Bambagioni, A. Ceccanti, D. Donati, G. Giorgi, M. Fontani, F. Laschi, P. Zanello, M. Casolaro, A. Pietrangelo, *J. Med. Chem.* **2002**, *45*, 5776−5785.
[32] M. Comporti, A. Hartman, N. R. Di Luzio, *Lab. Invest.* **1967**, *16*, 616−624.
[33] Z. D. Liu, R. C. Hider, *Coord. Chem. Rev.* **2002**, *232*, 151−171.

Received July 15, 2003
Early View Article
Published Online December 19, 2003

